Structural and electronic properties of the liquid polyvalent elements. II. The divalent elements

W. Jank and J. Hafner
Institut für Theoretische Physik, TU Wien, Wiedner Hauptstrasse 8-10, A-1040 Wien, Austria
(Received 30 April 1990)

We present *ab initio* calculations of the atomic structure, the electronic density of states (DOS), and the photoemission spectra of the divalent metals in the liquid state. Our approach is based on pseudopotential-derived interatomic forces, on molecular-dynamics simulations for the atomic structure, on self-consistent linear-muffin-tin-orbital supercell calculations for the electronic structure, and on a single-scatterer final-state approximation for the photoelectron spectrum. We show that both the atomic and the electronic structure of the IIB elements are influenced by relativistic effects: The damping in the Friedel oscillations in the interatomic potential induced by relativistic corrections leads to the characteristic distortion of the liquid structures of Zn, Cd, and Hg, and the relativistic increase of the *s-p* splitting enhances the structure-induced minimum in the electronic DOS at the Fermi level. The electronic structure of the alkaline-earth metals is dominated by the incipient occupation of the *d* band. Liquid Ba shows clear transition-metal behavior in the interatomic forces and in the electronic spectrum.

I. INTRODUCTION

Textbooks[1-3] on liquid metals generally agree in describing the electronic density of states (DOS) of the liquid simple metals as essentially free-electron-like. Greater interest has been aroused only in the study of the density of states of liquid Hg since Mott[4,5] introduced the concept of the pseudogap to account for its anomalous electronic properties. According to Mott's model the DOS at the Fermi level for liquid Hg should be about 30% lower than the free-electron value. A number of studies[6-9] has been devoted to the investigation of the correlation between the atomic structure of the liquid metal and the electronic DOS. It has been shown that essentially the peak in the static structure factor $S(q)$ at $q = |\mathbf{Q}_p|$ induces a DOS minimum at an energy (in atomic units) of $(\mathbf{Q}_p/2)^2$ above the bottom of the band. For an electron-per-atom ratio of about 2, we have $|\mathbf{Q}_p| \sim 2k_F$ and the structure-induced DOS minimum is expected at the Fermi energy E_F.[9,10] However, the quantitative predictions derived from the various models are widely different and until recently it has hardly been possible to test the predictions against experiment because of the lack of reliable spectroscopic information on the liquid metals.

This situation is now gradually changing. Important progress has been realized in the preparation of atomically clean liquid surfaces, making accurate photoemission investigations of the electronic spectrum of the liquid metals possible for the first time.[11-13] For liquid Hg the most recent photoemission experiments[11] confirm Mott's predictions rather well. For the theorist the challenge is to find a way of calculating the electronic structure of liquids, which accounts not only for the full information on the average atomic arrangement in the liquid, but also for the effect of the local fluctuations in the atomic correlations on the electronic structure. This means that the proper technique for calculating the electronic structure should achieve self-consistency locally, at every atomic site. To date the only technique to achieve this goal is the supercell technique:[10,14-18] The electronic structure is calculated for atoms arranged in a periodically repeated "supercell," using **k**-space techniques. The coordinates of the atoms within the cell are generated via molecular-dynamics (MD) or Monte Carlo computer simulation. As the minimum number of atoms in a supercell to constitute a realistic model of a liquid metal is 60 or more, the calculation of the electronic structure is a nontrivial task. Two different ways of solving the problem have been proposed: One consists in using a minimum basis-set technique such as the linear-muffin-tin-orbital (LMTO) method and proceeds by direct diagonalization of the resulting Hamiltonian matrix[10,14-17] (which is of the order 600 × 600). The second employs a plane-wave basis set (with up to 7000 plane waves to obtain a fully converged solution). In this case the solution of the one-electron Schrödinger equation can be found by a global minimization of the total energy via a dynamical-simulated-annealing[18] (DSA) procedure. For liquid metals with *s*- and *p*-state valence states only both techniques yield equivalent results.[18] The main advantage of the DSA approach is that the same pseudopotential can be used in the calculation of the interatomic forces employed in the MD simulation of the atomic structure and in the DSA calculation of the electronic structure. Ultimately convergence in the ionic equations of motion and in the one-electron wave equations may be sought simultaneously, combining MD and DSA to form a set of mixed classical quantum-mechanical equations of motion for both electronic and atomic degrees of freedom.[19-22]

The drawback is that for d states a plane-wave expansion converges rather badly, so that to date a DSA approach (which works only for local or semilocal pseudopotentials) is inapplicable to liquid metals with a substantial d character in the valence states. Now for all divalent metals except for Be and Mg there is some s-d hybridization in the valence band: in the IIA metals Ca, Sr, and Ba there is an increasing overlap of the s-band with an empty d band just above the Fermi level, in the IIB metals Zn, Cd, and Hg the filled $(n-1)d$ band overlaps with the bottom of the n-s band. For this reason the electronic structure calculations presented in this paper are based on the LMTO-supercell technique which previously has been used successfully for liquid metals[16,17] and amorphous alloys.[10,14,15,23]

Our paper is organized as follows. In Sec. II we recapitulate rather briefly the calculation of the interatomic forces using pseudopotential techniques and demonstrate the variation of the interatomic interactions induced by relativistic effects in the heavy metals, and by an increasing d-band occupancy in the heaviest alkaline-earth metals. In Sec. III we present the results of our MD simulations of the liquid metals and show how relativistic and d-electron effects influence the atomic structure. In Sec. IV we present, after a brief discussion of the technical aspects of the LMTO-supercell method, our results for the electronic densities of states for the crystalline and liquid metals. The calculated photoemission intensities are discussed in Sec. V, and the conclusions are presented in Sec. VI.

II. INTERATOMIC FORCES

The calculation of the effective interatomic potential using second-order pseudopotential perturbation theory is a standard procedure.[24–26] One only has to specifiy the choice of a pseudopotential and of the local-field corrections to the dielectric function in the random-phase approximation. For the local-field corrections we used the Vashishta-Singwi[27] form which satisfies the compressibility sum rule for the electron gas. Calculations using the Ichimaru-Utsumi[27] local-field corrections produce almost identical results. Hafner and Heine[28] have shown that even the simplest possible form of a pseudopotential (i.e., the empty-core pseudopotential proposed by Ashcroft[29]) allows for a very convincing analysis of the variations in the effective interatomic interactions with electron density and pseudopotential across the Periodic Table, and for an at least semiquantitative analysis of the trend in the crystalline[28,30] and liquid structures.[30,31] However, our previous molecular-dynamics studies of the structure of the liquid tetravalent metals[17] (hereafter this paper will be referred to as I) have shown that the quantitative description of the small departures of the liquid structure factor from a hard-sphere form in tin and the return to an essentially hard-sphere-like structure in Pb is a more delicate problem than the description of the massive short-range order effects in the lighter elements Si and Ge. In particular, we found it necessary to include at least a relativistic description of the ionic core into the pseudopotentials.

In the divalent liquid metals the trend in the structure is characterized by a progressive asymmetry of the static structure factor as the atomic number increases. Evidently a correct prediction of these delicate structural effects requires very accurate pair interactions. In the present work we have adopted the first-principles optimized pseudopotentials originally developed by Harrison[24] and used extensively in slightly different variants by Hafner,[26,30] Moriarty,[32–34] and others. In this approach exchange and correlation between the core electrons and the core valence exchange and correlation interactions are described in a local-density-functional framework.[35] In the nonrelativistic limit the core wave functions are calculated using the Herman-Skillman program,[36] the relativistic core orbitals are calculated using the scalar relativistic program of Koelling. For any further details see, e.g., Ref. 26.

Figure 1 shows the effective interatomic pair potential $\Phi(R)$ for the divalent metals from Be to Hg. Be has a very nonlocal pseudopotential with a strongly attractive p component. The strong electron-ion interaction leads to a very high density. As a consequence of the high electron density the first attractive minimum close to the nearest-neighbor distance is quite shallow, the minimum is partially covered by the repulsive core (cf. the detailed discussion in Hafner and Heine[28,36]). The long-range Friedel oscillations are quite pronounced, corresponding to a large on-Fermi-sphere matrix element of the pseudopotential. Mg has a nearly local pseudopotential, with a main minimum close to the nearest-neighbor distance in a close-packed (crystalline or liquid) configuration and strongly damped Friedel oscillations. In the IIB metals Zn, Cd, and Hg the presence of the d shell in the core leads to a volume contraction so that the atomic radius of Hg is about the same as that of Mg. In the nonrelativistic simple-metal limit the effective pair potential of the IIB metals looks very much like that of Mg. In the relativistic simple-metal limit the states of s character are lowered in energy with respect to those of p and d symmetry, leading to a reduction of the on-Fermi-sphere matrix element of the pseudopotential and hence to a strong damping of the Friedel oscillations in the pair potential. For Cd and Hg the pair interaction is purely repulsive around the nearest-neighbor distance, with a very small curvature in Hg. This confirms the arguments presented by Hafner and Heine,[28] except that the damping of the Friedel oscillations (the "amplitude effect") seems to be more pronounced than anticipated in their simple analysis.

The phase stability of the crystalline polymorphs of Hg has recently been discussed by Moriarty.[34] He showed that in the nonrelativistic simple-metal limit Hg has a hexagonal-close-packed (hcp) structure with a near ideal c/a ratio. Including relativistic effects in the calculation of the core orbitals, or including the hybridization of the

filled $5d$ shell with the valence band, leads to a distorted hcp structure with a large c/a ratio. However, only if both relativistic effects and d-band effects are included, the observed body-centered tetragonal (bct) structure is stabilized.[34] The effective pair interaction calculated by Moriarty is very close to the one derived in the present work in the relativistic simple-metal limit (Fig. 1), except for an even smaller curvature in $\Phi(R)$.

Relativistic effects are also important in understanding the properties of the heavy alkaline-earth metals Ca, Sr, and Ba, but here we find that the situation is further complicated by a partial d-band filling leading to a transition-metal behavior at least in Ba. For the crystalline metals phase stability and phonon spectra have been investigated in detail by Moriarty.[33,37] He shows that for Ca and Sr a simple-metal treatment is essentially adequate, but sp-d hybridization is essential to lower the phonon frequencies close to the experiment. For Ba a simple-metal treatment fails. Self-consistent LMTO calculations[38] indicate that there is nearly one d electron per atom in Ba. Hence Ba should be treated as a transition metal. Indeed Moriarty's generalized pseudopotential perturbation theory[39] (GPPT) leads to accurate phonon frequencies for Ba.[33] An alternative way to arrive at realistic interatomic forces in metals with nearly free s electrons and tightly bound d electrons is the hybridized nearly-free-electron–tight-binding-bond (NFE-TBB) approach originally proposed by Wills and Harrison[40] and recently modified[41] and extended to binary transition-metal alloys by Hausleitner and Hafner.[42]

Figure 2 shows the pair potentials for Ca, Sr, and Ba

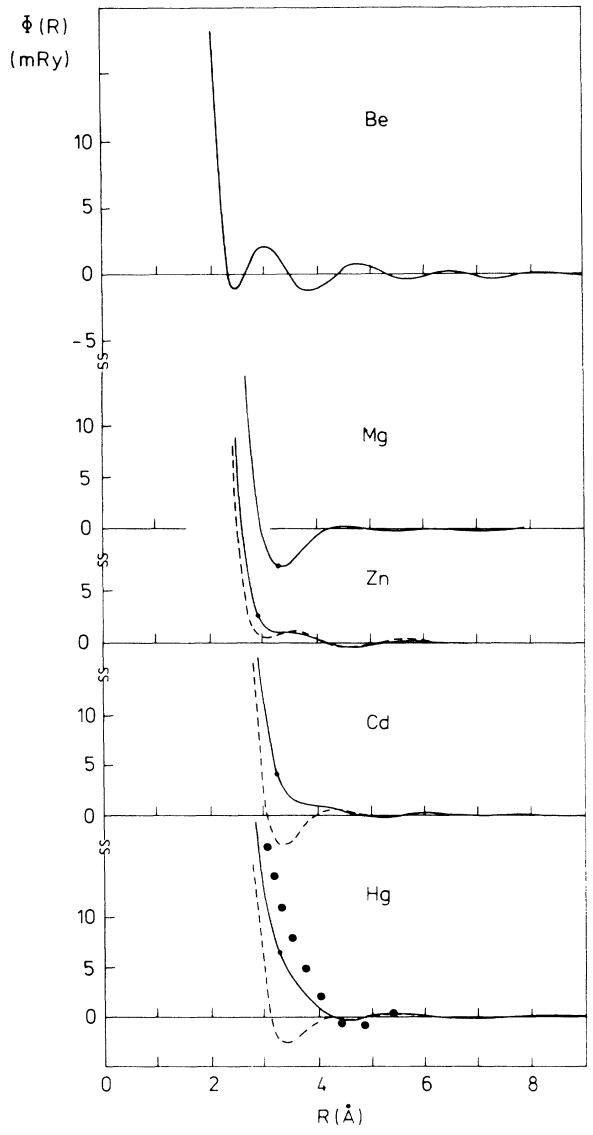

FIG. 1. Interatomic pair interaction $\Phi(R)$ for the divalent liquid metals from Be to Hg. Solid line, simple-metal calculation with relativistic core; dashed line, simple-metal calculation with nonrelativistic core (both results are indistinguishable for Be and Mg). Dotted line, generalized pseudopotential calculation (filled d band) for Hg after Moriarty (Ref. 34). The open circles mark the nearest-neighbor distance D_{cp} for close packing (see text).

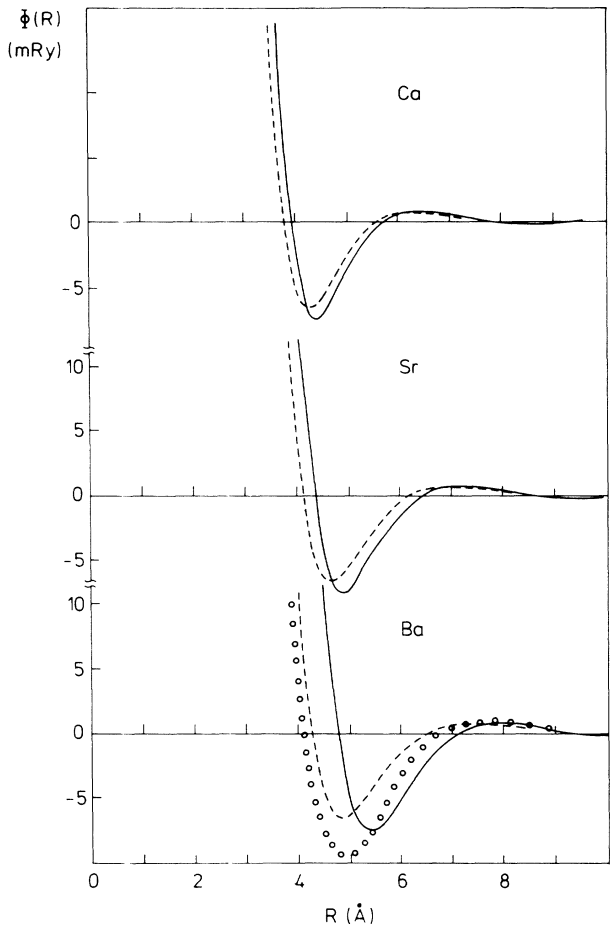

FIG. 2. Interatomic pair interaction $\Phi(R)$ for the liquid alkaline-earth metals from Ca to Ba. Solid line, relativistic core; dashed line, nonrelativistic core in the simple-metal limit. Open circles, generalized pseudopotential calculation by Moriarty (Ref. 39), treating Ba as a transition metal with 0.75 d electrons per atom (see text).

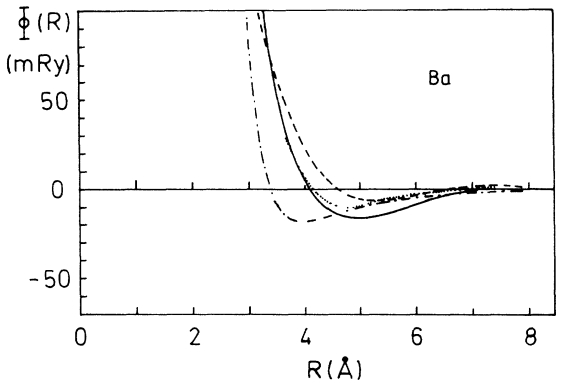

FIG. 3. Interatomic pair interaction $\Phi(R)$ (solid line) for liquid Ba, calculated using hybridized pseudopotential tight-binding-bond theory, decomposed into s- (dashed line) and d- (dash-dotted line) electron contributions. The generalized pseudopotential calculation by Moriarty (Ref. 33) is shown for comparison (dotted line).

calculated in the nonrelativistic and relativistic simple-metal limits; for Ba we show in addition the results obtained by Moriarty[39] in the generalized pseudopotential theory for transition metals and that derived from NFE-TBB theory (Fig. 3). Both calculations are based on $Z_s = 1.25$ s and $Z_d = 0.75$ d electrons in Ba; the NFE-TBB approach assumes a d-band width of W_d=7.0 eV and an average d-d transfer integral $h(R_o)$=0.6217 eV at the nearest-neighbor separation in the crystal. For a more detailed discussion of the NFE-TBB method we refer to the articles by Hausleitner and Hafner.[41,42] The relativistic effects lead to a slightly expanded repulsive part of the potential and slightly larger Friedel oscillations. At least for Ba including the relativistic effects definitely worsens the agreement with experiment for phonon frequencies, phase stability, liquid structure, etc. The explanation is that covalent d-bonding effects lead to an additional attractive interaction which overcompensates the relativistic effects. For the NFE-TBB potential a decomposition of the pair potential into s- and d-electron contribution is shown in Fig. 3. Note that both transition metal treatments (GPPT and NFE-TBB) lead to reasonably consistent results for the pair interactions in Ba. In the following we discuss the calculation of the liquid structure on the basis of these pair interactions.

III. ATOMIC STRUCTURE

The calculation of the atomic structure is based on a conventional molecular dynamics algorithm; for any details we refer to I and to earlier publications.[43,44] Two sets of calculations were performed: simulations on large ensembles (N=512–1372 atoms) served to create pair-correlation functions and static structure factors to be compared with experiments; simulations with 64 atoms per molecular-dynamics cell served to create the coordinates needed as the input to the electronic structure calculations.

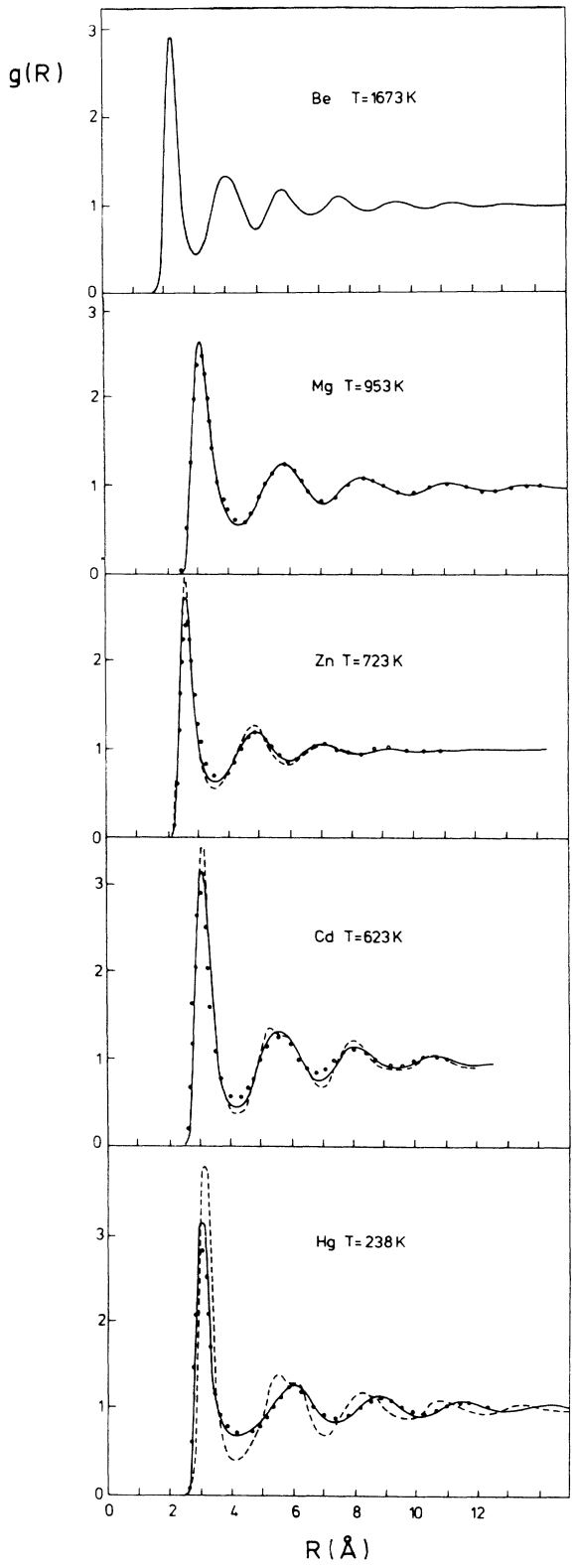

FIG. 4. Pair correlation function $g(R)$ for the divalent metals from Be to Hg. Solid line, MD calculations using the pseudopotentials based on relativistic core orbitals; dashed line, MD calculations based on nonrelativistic pseudopotentials (for Be and Mg there is now difference between both calculations). Open circles, diffraction data (after Ref. 52).

Figures 4 and 5 show the pair-correlation function $g(R)$ and the static structure factor $S(q)$ for the divalent metals Be to Hg, calculated with the relativistic and nonrelativistic simple-metal pair interactions. (Input data for all calculations are given in Table I. The densities are taken from experiment. Densities can in principle be calculated *ab initio*, with an accuracy of typically 5% in the crystalline state.[26] For the liquid this sort of calculation would multiply the computational effort without giving essential new information.) As shown by a series of x-ray and neutron-diffraction investigations,[45–52] the structures of the divalent metals show an increasing departure from a hard-sphere model with increasing atomic number. The most pronounced manifestations of this trend are the asymmetry of the first peak in $S(q)$ observed in Zn and Cd, and the shoulder in the first peak of $S(q)$ in Hg. Note that this trend in the liquid structure parallels the increasing distortion of the axial ratio in the hcp structures of Zn and Cd, culminating in a unique bct structure in Hg. We find that with the relativistic pair interactions our molecular-dynamics simulations describe the distorted structure very well. The nonrelativistic pair interactions for Zn, Cd, and Hg, on the other hand, look very much like those in Mg. In the MD simulations with these potentials we find that the crystalline starting structures melt only at temperatures that are several hundered degrees higher than the observed melting temperature. The structures produced by melting at high temperature and subsequent cooling look very much like strongly supercooled hard-sphere liquids or hard-sphere glasses [see the split second peak in $g(R)$ for Cd and Hg in Fig. 4]. This shows that the relativistic effects in the pair interactions are important not only for the understanding of the anomalous liquid structures of the IIB metals, but also of their unusual low melting points.

TABLE I. Input data for the calculations: atomic volume V_s and V_l for the solid and liquid phases and temperatures T (K) of the melts.

	V_s (Å^3)	V_l (Å^3)	T (K)
Be	8.089	8.863	1573
Mg	23.231	26.114	953
Zn	15.206	15.698	723
Cd	21.579	23.464	623
Hg	22.981	24.579	238
Ca	43.632	48.573	1123
Sr	56.300	61.335	1053
Ba	62.989	68.477	1003

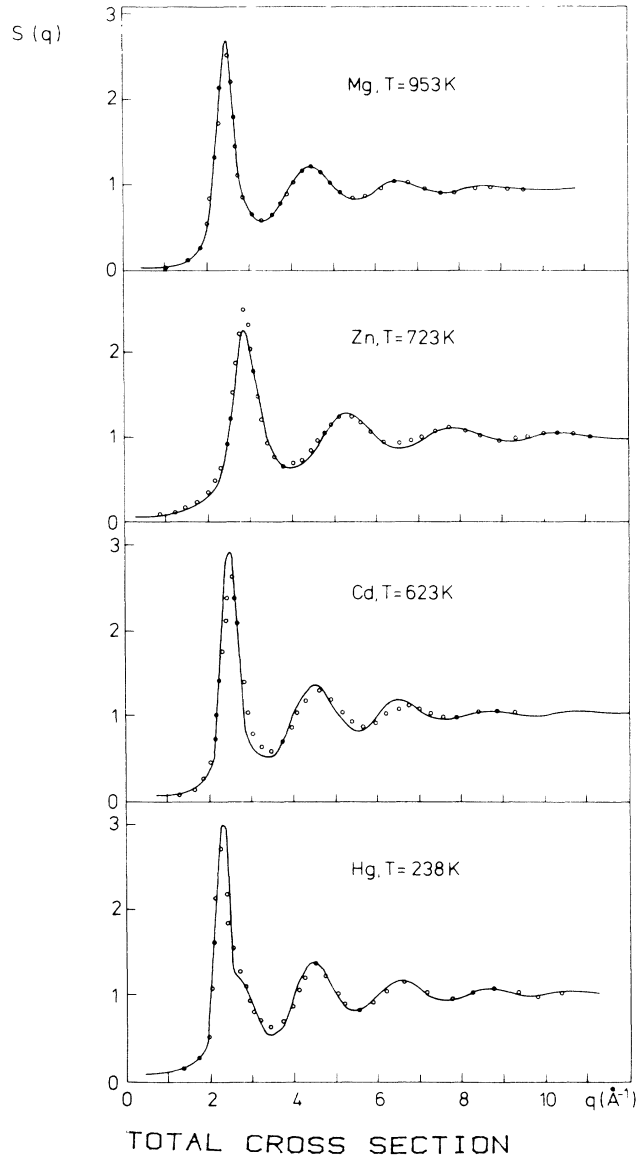

FIG. 5. Static structure factor $S(q)$ for the divalent metals from Mg to Hg. Solid line, theory (using the relativistic pseudopotentials; see text); open circles, diffraction data (after Ref. 52).

The physical mechanism leading to these distorted structures is the same as that which leads to the open structures of the liquid elements from groups IV to VI, i.e., a modulation of the random packing of the atoms by the Friedel oscillations in the interatomic potentials. The occurrence of such a distortion depends (a) on a deviation of the nearest-neighbor distance D_{cp} in a regular close-packed structure from the position of the first minimum in $\Phi(R)$, and (b) on the amplitude of the oscillations. In I we have shown that (a) leads to the formation of open structures with low coordination numbers in Si and Ge, while the damping of the oscillations (b) leads to a return to close-packed metallic structures in the heavy elements Sn and Pb. In the divalent elements we find that both effects play a role only for the heavier IIB elements; the damping of the oscillations limits the distortion of the structure. Our computer-simulation studies confirm and extend our previous analysis of the crystalline and liquid structures, in particular our argument that the reduction of the pseudopotential core radius simulates the relativis-

tic effects in the electron-ion interaction.

Figure 6 shows the pair correlation functions for liquid Ca, Sr, and Ba. For the heavy alkaline-earth metals the nonrelativistic simple-metal pair interactions lead to a reasonably accurate description of the liquid structure, albeit with a tendency to overestimate the amplitude of the first peak. The inclusion of relativistic effects does not improve the accuracy of the predictions—to the contrary: there is a tendency to overstimate the melting temperature as long as the calculation is performed in the simple-metal limit. An MD simulation of liquid Ba with the NFE-TBB pair interaction, on the other hand, yields good agreement with experiment. Thus our investigation of the structure of liquid Ba supports the conclusion based on Moriarty's study of the vibrational properties of crystalline Ba:[33] Ba behaves as an early transition metal, with the $5d$ band partially occupied and strongly influencing the interatomic forces. On the whole, our MD study shows that with proper considerations of relativistic effects in the heavy metals *and* of d-electron bonding in Ba, the pseudopotential-derived interatomic forces lead to an adequate description of the atomic structure of the divalent metals.

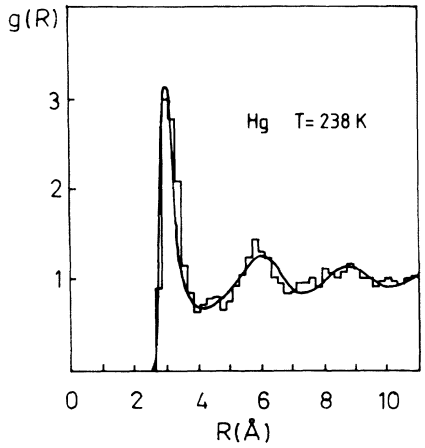

FIG. 7. Pair-correlation function for liquid Hg. Solid line, configuration average over a 512-atom ensemble; histogram, calculated for a single 64-atom configuration used in the electronic structure calculation.

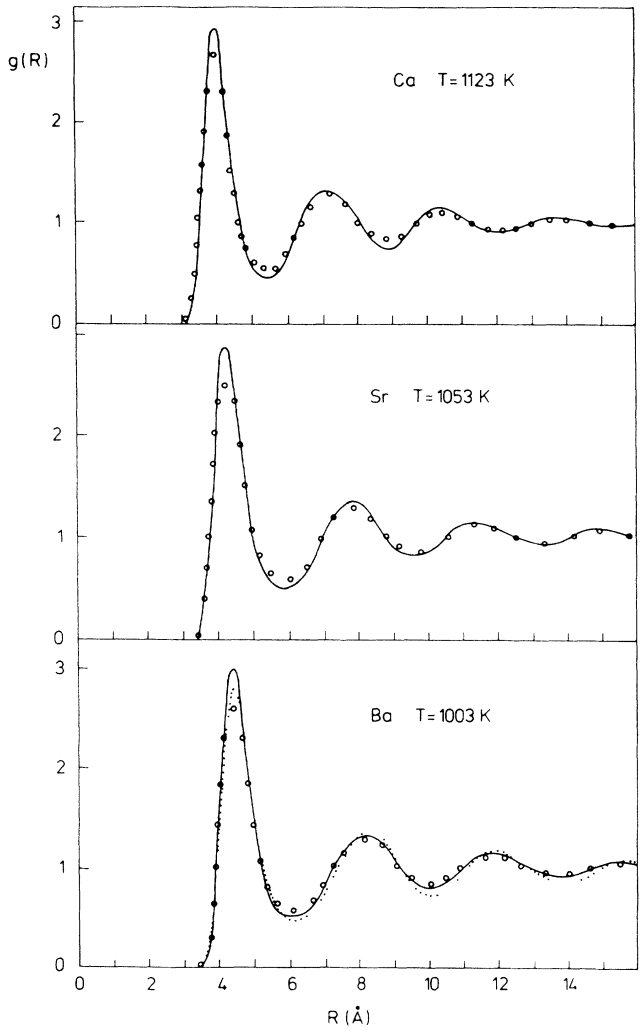

FIG. 6. Pair-correlation function $g(R)$ for the alkaline-earth metals Ca, Sr, and Ba. Solid lines, MD calculations using the nonrelativistic pseudopotentials; dotted line, MD calculation using the NFE-TBB pair potential for the "transition metal" Ba; open circles, diffraction data (after Ref. 52).

As in I we find that the simulations using the small $N=64$ ensembles reproduce the correlation functions of the large ensembles quite well—a characteristic example for the delicate case of liquid Hg is shown in Fig. 7. This demonstrates that the 64-atom ensemble is a realistic basis for the electronic structure calculations.

IV. ELECTRONIC STRUCTURE

The technical aspects of the supercell calculations of the electronic density of states based on the LMTO technique[53,54] have been discussed in I. Here we shall comment only on two special points. The first concerns the **k**-point sampling necessary for the construction of the charge density and of the DOS. In I we have pointed out that, due to the limited size of the supercell and the rather large band width characteristic for sp-bonded elements, the DOS is not very well described by the eigenvalues of a single **k** point (usually the Γ point). We have proposed two alternatives, a sampling of the Brillouin zone (BZ) belonging to the supercell on a regular grid of up to 10 **k** points or the use of the special point scheme of Baldereschi.[55] In both cases we used only **k** points in the irreducible part of the simple-cubic Brillouin zone. This is not entirely correct. The supercell model possesses the translational symmetry of a simple-cubic lattice, but not its point-group symmetry. This means that the sampling should be over the entire Brillouin zone. However, if we proceed to this extended **k**-space sampling, we find only a very small difference between the DOS based on four points in the irreducible part of the BZ and the DOS

calculated from the complete set of 32 points (see Figs. 8–15). This shows that the results presented in I remain valid within the limited statistical accuracy that can be achieved for these relatively small cells. The second point concerns the configuration averaging. In I we have emphasized that although there are quite large fluctuations in the local DOS's, the configuration dependence of the total DOS is weak except for localized resonant bound states at low energy, which may appear if the selected configuration contains very short interatomic distances (arising from thermal fluctuations) and if the potential parameters allow for rather extended d orbitals. In the real material such short-lived resonances contribute to the low-energy tail of the DOS; in the supercell calculation they can cause a rather slow convergence. These resonances can be partially eliminated by fixing the reference energy for the d states at a sufficiently high energy. This procedure has been used for Be and Mg.

A. Beryllium

The electronic structure of crystalline hcp Be (Fig. 8) is characterized by a deep structure-induced minimum in the DOS (almost a gap) at the Fermi level. At the Fermi energy the DOS is reduced to 30% of its free-electron value. Due to large amplitudes of the DOS at binding energies between 2 and 8 eV, the bandwidth is reduced to W=11.25 eV compared to a free-electron bandwidth of W_{FE}=14.35 eV. The same structure-induced features subsist in the liquid state, only the DOS minimum is flattened. The DOS at the Fermi level is now 70% of the free-electron value. In the crystalline case it is well known that the DOS minimum at E_F originates from large gaps at the L and H point whose width is directly proportional to the $\mathbf{Q}(1001)$ and $\mathbf{Q}(1101)$ matrix element of the pseudopotential. The origin of the deviation from the free-electron model in liquid Be is essentially the same: The sharp first peak of the static structure factor at Q_p=3.38 Å^{-1} acts as a smeared-out reciprocal lattice vector and induces a DOS minimum at an energy of $(\mathbf{Q}_p/2)^2$=10.9 eV above the bottom of the band. The width of the pseudopap is given by the product of the structure factor and the modulus of the pseudopotential matrix element proportional to $2S(\mathbf{Q}_p)|w(\mathbf{Q}_p)|$. Hence the existence of a pseudogap in liquid Be is related to the large amplitude of the structure factor (which is a consequence of the high packing density) and the strength of the pseudopotential (which is due to the fact that the p states feel the full electron-ion potential). From the partial DOS we find that the s states are concentrated at the lower half of the conduction band, with the states at the Fermi level being predominantly of p character.

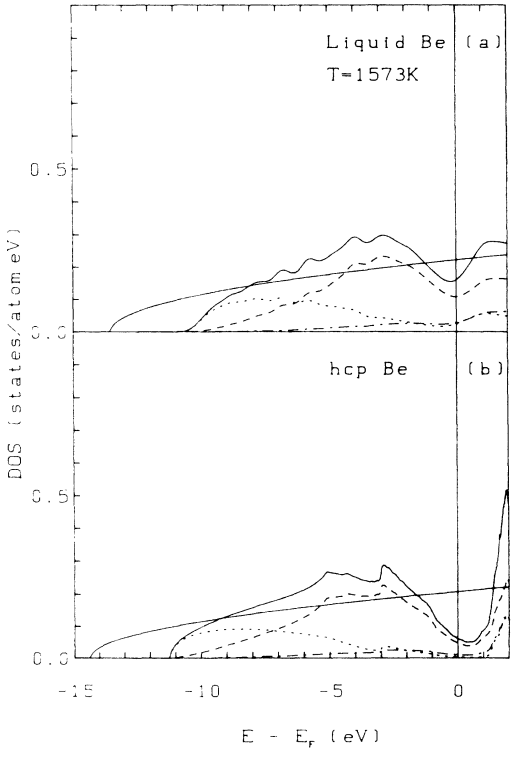

FIG. 8. Electronic density of states for (a) liquid and (b) crystalline hcp Be. Solid line, total DOS; dotted line, s states; dashed line, p states; dash-dotted line, d states. The parabola shows the free-electron DOS.

B. Magnesium

The electronic DOS of hcp Mg (Fig. 9) shows the same structure-induced features, but they are now much

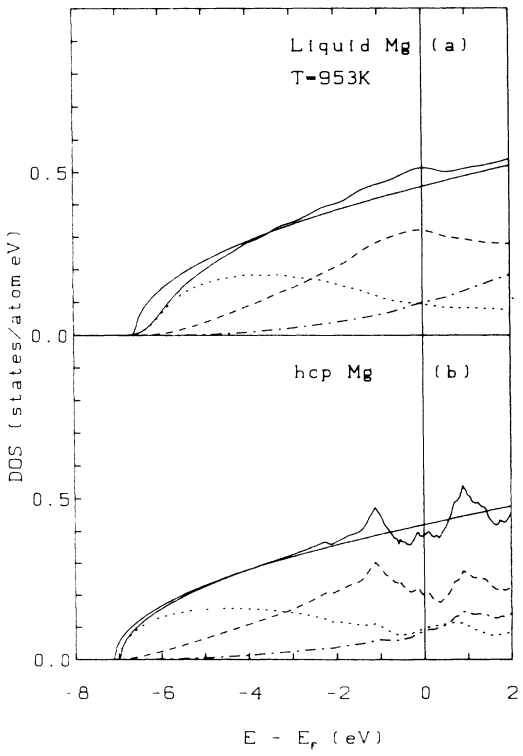

FIG. 9. Electronic density of states for (a) liquid and (b) crystalline hcp Mg. For meaning of symbols, see Fig. 8.

weaker than in Be—as expected. The DOS of liquid Mg is essentially free-electron-like, except for a slight reduction of the bandwidth (W=6.2 eV if we ignore the small tail resulting from the Gaussian broadening, against W_{FE}=6.6 eV).

C. Zinc, cadmium, and mercury

The electronic DOS's of hcp and liquid Zn, Cd, and bct and liquid Hg are shown in Figs. 10–12. The common features of the crystalline metals are a narrow d band overlapping with the bottom of a broad sp band and a structure-induced DOS minimum at E_F. The degree of overlap between the sp and d bands is influenced by the atomic volume and relativistic effects. The small volume of Zn leads to a very broad sp band and a strong sp-d hybridization, whereas at the larger atomic volume of Cd we find only a weak sp-d overlap. In Hg the s states are lowered relative to the d states by relativistic effects and this leads again to a much larger band overlap. In the liquid state we observe a broadening of the d band (most pronounced in liquid Zn) and a smearing-out of the structure-induced features in the DOS. However, substantial deviations from a free-electron parabola subsist in the heavy metals. The g factor introduced by Mott [$g \equiv n(E_F)/n_{FE}(E_F)$] is g=0.9, 0.86, and 0.73 in l-Zn, l-Cd, and l-Hg. This is in rather good agreement with the photoemission results of Indlekofer *et al.*,[12,56] suggesting $g = 0.80 \pm 0.03$ for l-Hg.

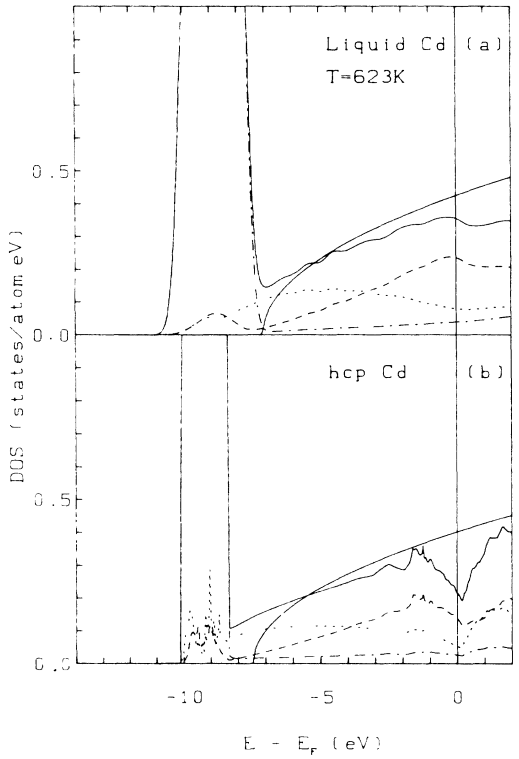

FIG. 11. Electronic density of states for (a) liquid and (b) crystalline hcp Cd. For meaning of symbols, see Fig. 8.

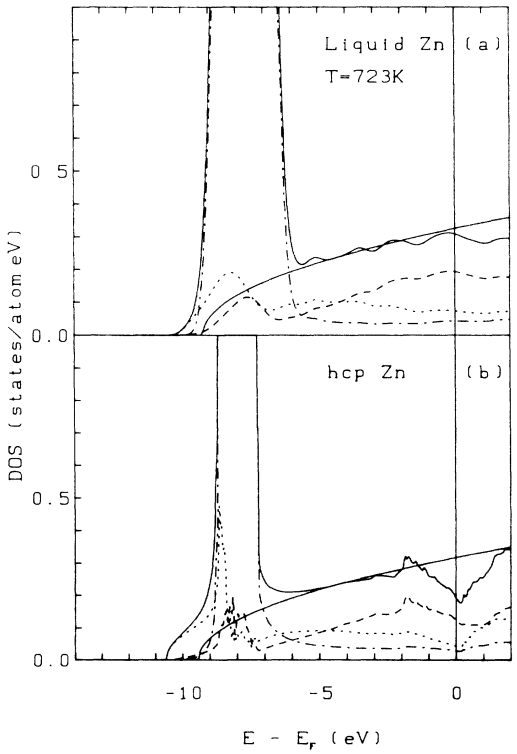

FIG. 10. Electronic density of states for (a) liquid and (b) crystalline hcp Zn. For meaning of symbols, see Fig. 8.

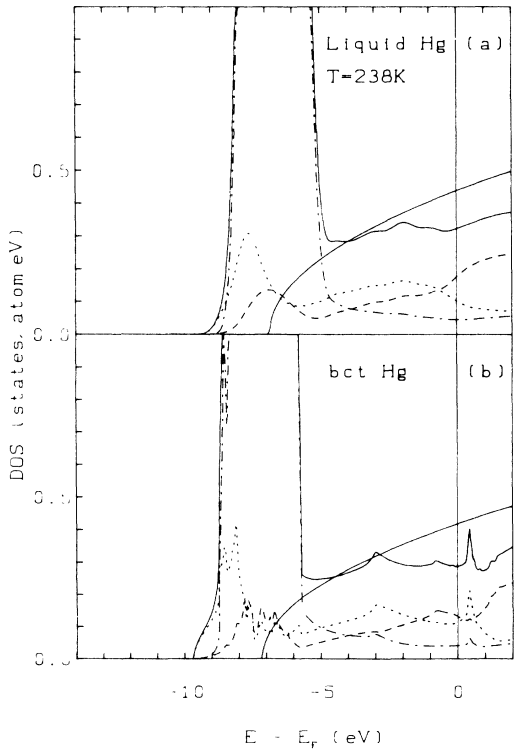

FIG. 12. Electronic density of states for (a) liquid and (b) crystalline bct Hg. For meaning of symbols, see Fig. 8.

The trend in $n(E_F)$ is related to the amplitude of $S(q)$ (see Fig. 5) and to a decreasing s-p hybridization: Relativistic effects tend to lower the s-states not only to the d, but also relative to the p states. This parallels the trend in the tetravalent metals discussed in I, where relativistic effects lead to a formation of separate s and p bands. However, even in Hg the partial densities of states point to an appreciable s-p hybridization. Our calculations predict a p band that is broader and contains more electrons than has been suggested from an analysis of the trends in the photoemission spectra.[12,56] A careful comparison of our results with the existing photoemission data requires also a determination of the partial photoionization cross sections; see Sec. V.

D. Calcium, strontium, and barium

The electronic structure of the alkaline-earth metals Ca, Sr, and Ba is complicated by the presence of an empty d band just above the Fermi level. As we have pointed out in Sec. II, a partial occupation of the d band has a pronounced influence on the interatomic interactions and hence on the structure of the liquid. The precise character of the electronic DOS at the Fermi level is also important for the electronic transport properties. Two conflicting explanations for the anomalous high electrical resistivity of liquid Ba ($\rho \sim 306\ \mu\Omega$ cm close to the melting point) have been proposed: the d-resonance model[57] and a pseudogap model[9] relating the increase in the resistivity to the reduction of the electronic DOS at the Fermi level.

Figures 13 to 15 show the electronic DOS of crystalline fcc and liquid Ca and Sr, and of crystalline bcc and liquid Ba. In the crystalline metals we find a rather substantial reduction of the width of the occupied band against the free-electron value (Ca: W=4.0 eV, W_{FE}=4.67 eV; Sr: W=3.70 eV, W_{FE}=3.95 eV; Ba: W=2.87 eV, W_{FE}=3.65 eV) and a strong admixture of d states at the Fermi level leading to an enhanced DOS for binding energies up to ~2 eV. In bcc Ba the Fermi level falls into a pronounced structure-induced minimum of the DOS. This structure arises from the d band and explains the stability of the bcc lattice over the fcc structure as already discussed by Skriver,[58] Moriarty,[33] and Chen, Ho, and Harmon.[59] The number of d electrons per atom is n_d=0.532, 0.591, and 0.872 in crystalline Ca, Sr, and Ba.

In the liquid alkaline-earth metals we find a more pronounced broadening of the DOS than in other liquid simple metals. The low-energy onset of the band is now quite far from a parabolic form—note that even in crystalline metals the free-electron parabola is a poor approximation. Including the low-energy tail we measure a bandwidth which is almost equal to the free-electron value. The d band loses all structure. In all three alkaline-earth metals the DOS at E_F is enhanced by a factor of 1.7 to 1.9 over the free-electron value. The difference between Ca and Sr at the one side and Ba

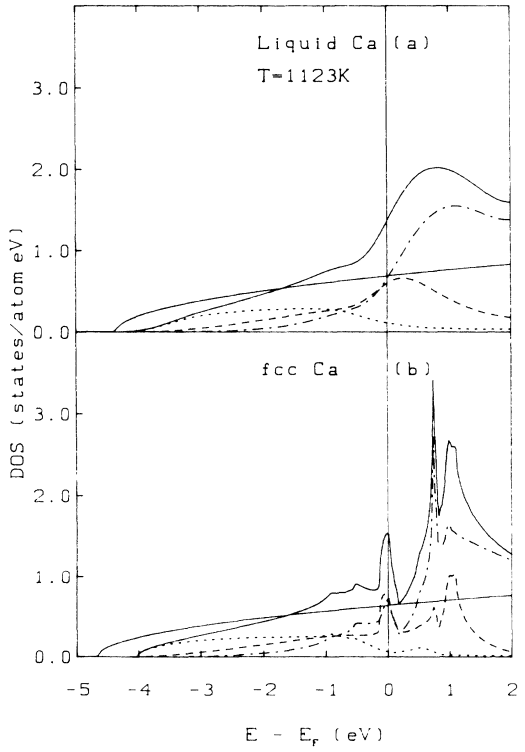

FIG. 13. Electronic density of states for (a) liquid and (b) crystalline fcc Ca. For meaning of symbols, see Fig. 8.

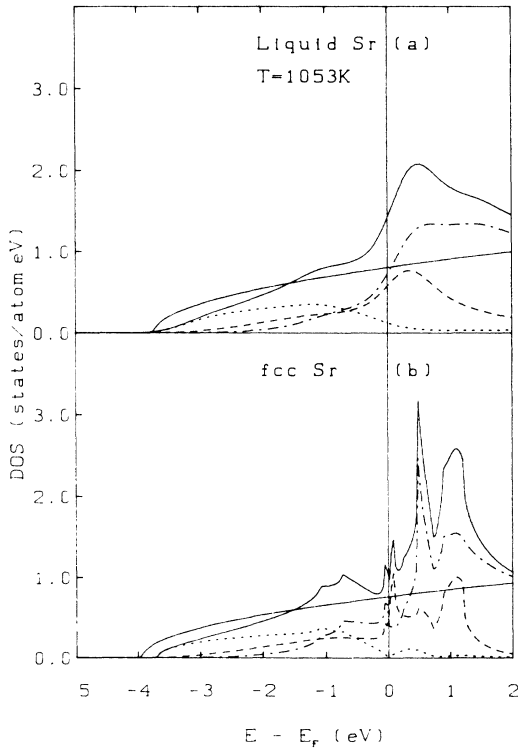

FIG. 14. Electronic density of states for (a) liquid and (b) crystalline fcc Sr. For meaning of symbols, see Fig. 8.

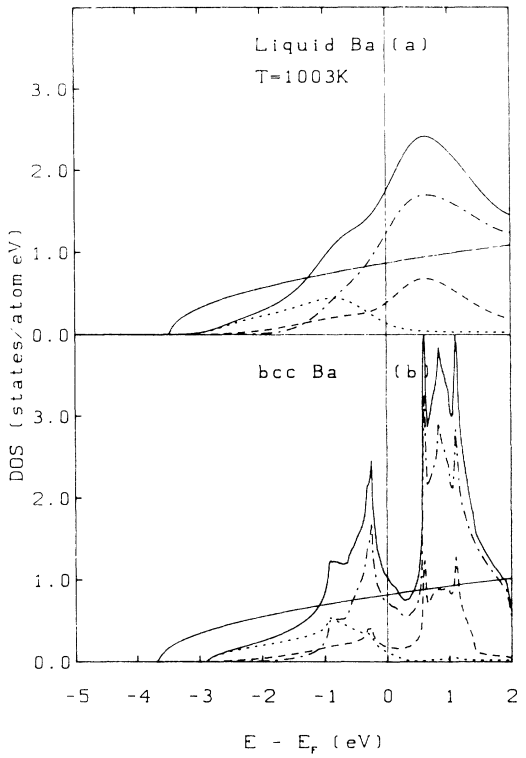

FIG. 15. Electronic density of states for (a) liquid and (b) crystalline bcc Ba. For meaning of symbols, see Fig. 8.

on the other side is not in the total, but in the partial DOS: In Ca and Sr we have about equal numbers of p and d electrons (n_s:n_p:n_d = 0.86:0.70:0.44 in Ca, n_s:n_p:n_d = 0.90:0.60:0.50 in Sr), whereas in Ba the number of d electrons is enhanced at the expense of p states (n_s:n_p:n_d = 0.80:0.38:0.82 in Ba). Hence the calculation of the electronic structure confirms the transition-metal behavior of l-Ba.

The sum of the s and p DOS alone shows the minimum close to E_F predicted by van Oosten and Geertsma[9] using a pseudopotential Green's-function technique. In a realistic calculation, however, the minimum is nearly completely covered by the onset of d states.

V. PHOTOEMISSION INTENSITIES

The absence of any spectacular structure in the DOS complicates the comparison with measured photoemission spectra. Any detailed discussion must consider the excitation- and binding-energy dependence of the partial photoionization cross sections.[60] Under the following approximations the photoemission intensities can be calculated in terms of the self-consistent potentials and the partial DOS's: (a) complete neglect of wave-vector conservation, (b) single-scatterer final-state approximation, (c) dipole approximation for the photon field, (d) independent angular averages over polarizations and wave vectors of photons and emitted electrons.[60-62] In the crystalline case (a) restricts the approach to high excitation energies where phonon broadening relaxes wave-vector conservation. In the liquid state where the wave vector is not a conserved quantity, the approximation may be used as long as the energy difference is large enough so that initial and final states do not violate the selection rules.

Figure 16 shows the partial ionization cross sections $\sigma_l(E,\hbar\omega)$ for Mg as a function of the binding energy E and for different photon energies $\hbar\omega$, together with the photoemission intensites

$$I(E,\hbar\omega)=\sum_{l=0}^{2}\sigma_l(E,\hbar\omega)n_l(E)\ . \tag{1}$$

For energies corresponding to ultraviolet photoemission spectroscopy (UPS) the s and p cross sections are of comparable magnitude. This results in a triangular photoemission spectrum like the one in the case of liquid Na.[63] For x-ray photoemission spectra (XPS) the measured intensity is dominated by the s contribution and we find a more or less semielliptic distribution of the energy of the photoelectrons.

For Zn, Cd, and Hg an additional complication arises from the narrow d band. It is well known that at the end of the transition-metal series,[64] for the noble metals,[65]

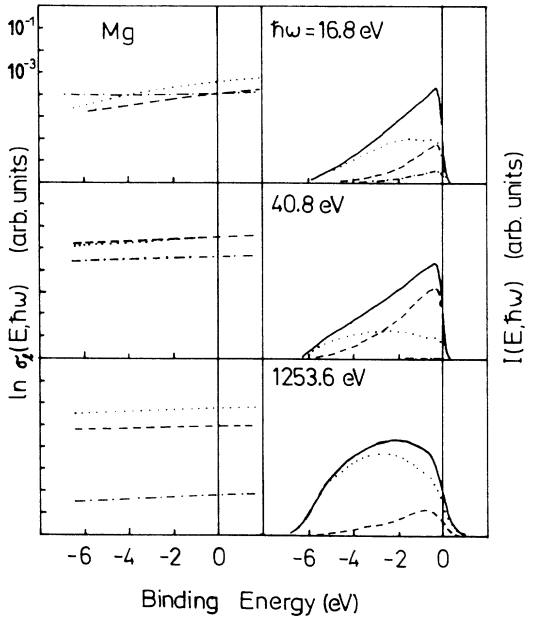

FIG. 16. Partial photoionization cross sections $\sigma_l(E,\hbar\omega)$ (dotted line, σ_s; dashed line, σ_p; and dash-dotted line, σ_d) and photoemission intensity $I(E,\hbar\omega)$ (solid line, total; dotted line, s-electron; dashed line, p-electron; and dash-dotted line, d-electron contribution) for liquid Mg at various energies of the exciting photon. For UPS energies the calculated intensity has been multiplied with a Fermi function; for the XPS spectrum the calculated intensity additionally has been Gaussian broadened (σ=0.50 eV) to account for the lower experimental resolution.

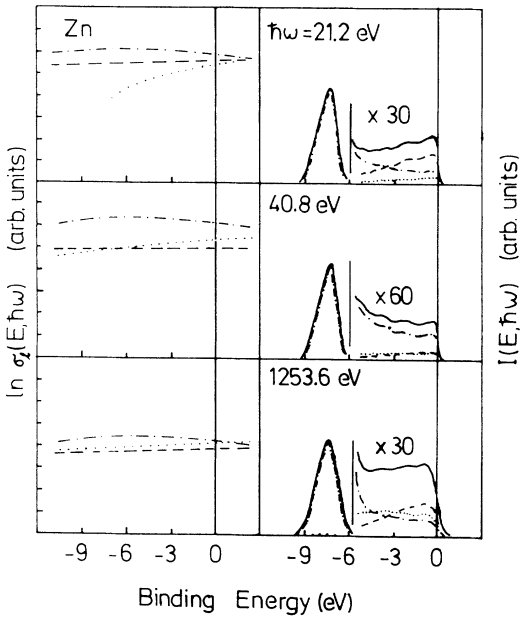

FIG. 17. Partial photoionization cross sections $\sigma_l(E,\hbar\omega)$ and photoemission intensity $I(E,\hbar\omega)$ for liquid Zn; cf. Fig. 16.

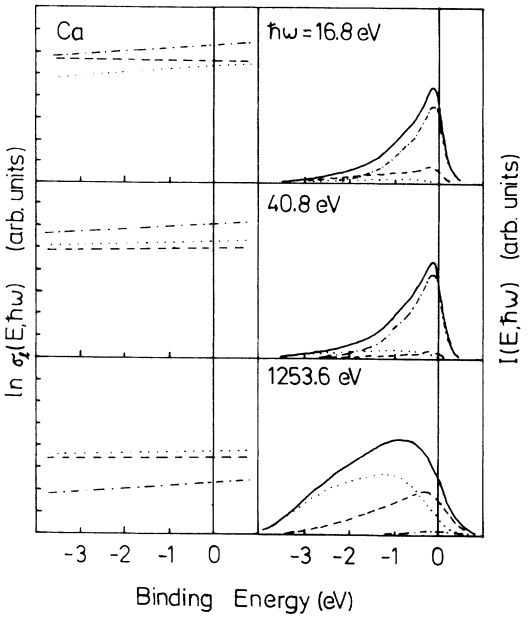

FIG. 19. Partial photoionization cross sections $\sigma_l(E,\hbar\omega)$ and photoemission intensity $I(E,\hbar\omega)$ for liquid Ca; cf. Fig. 16.

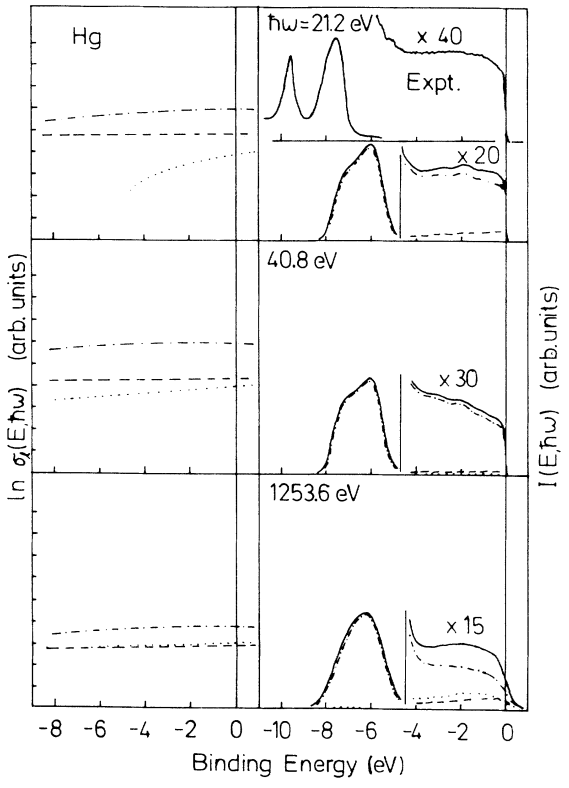

FIG. 18. Partial photoionization cross sections $\sigma_l(E,\hbar\omega)$ and photoemission intensity $I(E,\hbar\omega)$ for liquid Hg; cf. Fig. 16. The experimental results of Indlekofer *et al.* (Refs. 12 and 56) are shown for comparison.

and for the IIB metals,[66] the local-density approximation (LDA) yields d bands that are too high and too dispersive compared to photoemission data. For crystalline Zn and Cu it has been shown that self-interaction corrections (SIC) to the LDA lead to a shift of the d band to higher binding energies and to a reasonable d-band dispersion.[67] For Zn a self-consistent screened SIC calculation predicts

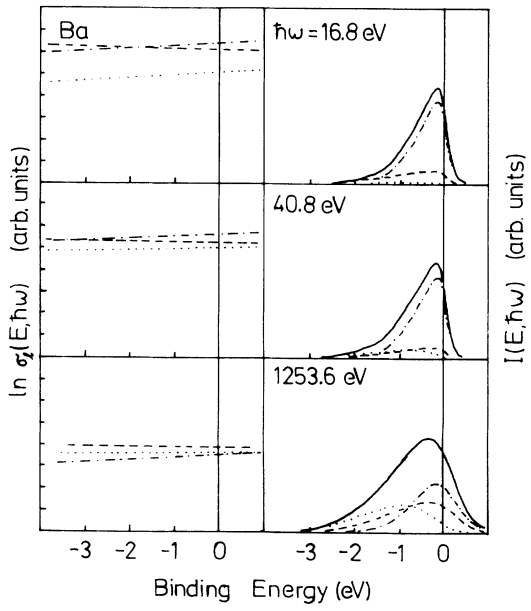

FIG. 20. Partial photoionization cross sections $\sigma_l(E,\hbar\omega)$ and photoemission intensity $I(E,\hbar\omega)$ for liquid Ba; cf. Fig. 16.

a shift of the d band by δ=2.53–2.58 eV. Based on a much simpler transition-state analysis, we have recently found a d-band shift by 2.4 eV in amorphous Mg-Zn alloys.[10]

The results for Zn and Hg (Figs. 17 and 18) show that the spectra are dominated by the d-electron contributions. The calculated d peaks have to be shifted by δ=2.3 eV for Zn and by δ=1.5 eV for Hg. For Hg the spin-orbit interaction (which is neglected in our scalar-relativistic version of the LMTO) leads to a splitting of the d band into $d^{3/2}$ and $d^{5/2}$ subbands. The s-p dominated part of the spectrum (up to about 4–5 eV binding energy) can be compared with the photoemission data of Indlekofer *et al.*[12,56] for Hg. The comparison shows our prediction for the DOS minimum at the Fermi edge to be quite realistic.

For the alkaline-earth metals the photoemission intensity is dominated at UPS energies by the d-electron contribution, at XPS energies the partial s and partial p DOS dominate the spectrum for l-Ca (Fig. 19). For l-Ba the XPS spectrum consists of about equal s, p, and d contributions (Fig. 20).

VI. CONCLUSIONS

We have presented *ab initio* calculations of the atomic and electronic structure, and of the photoemission intensities of the liquid divalent metals. For the IIB elements from Be to Hg we find structure-induced minima in the electronic density of states at an energy of approximately $(\mathbf{Q}_p/2)^2$ above the bottom of the band ($\mathbf{Q}_p$ is the wave vector corresponding to the main peak in the structure factor). The DOS minimum is quite pronounced in l-Be (g=0.70) due to the strong nonlocal pseudopotential, extremely weak in l-Mg, and increases in the sequence Zn (g=0.90), Cd (g=0.86), and Hg (g=0.73) due to relativistic effects. Relativistic effects are also found to be important for understanding the trends in the interatomic interactions and in the atomic structure. In this respect our study confirms and extends the general analysis of Hafner and Heine[28,30] and Hafner and Kahl[30,31] of the crystalline and liquid structure of the elements.

For the liquid alkaline-earth metals Ca, Sr, and Ba the trend in the electronic structure is dominated by the incipient occupation of the d band. We find n_d=0.44, 0.50, and 0.82 d electrons per atom in Ca, Sr, and Ba. In liquid Ba the electronic DOS at the Fermi level has 70% d character, and we confirm the conclusions reached by Moriarty[39] for crystalline Ba that the transition-metal character of this metal is important in the interatomic interactions and in determining its atomic structure.

The theoretical predictions for both the atomic and electronic structure are found to be in good agreement with experiment. For the atomic structure the agreement is almost within the accuracy of the experimental data. Only for l-Hg accurate photoemission data are available. The most important limitation to the theoretical prediction arises from the local-density-approximation: Self-interaction corrections shift the d band by about 2 eV relative to the LDA prediction. The photoemission intensity calculated for the sp band of Hg is in good agreement with experiment and confirms that our prediction for the DOS minimum is very realistic.

ACKNOWLEDGMENTS

We thank Dr. Ch. Hausleitner for calculating the NFE-TBB pair interaction for l-Ba and Professor P. Weinberger and Dr. J. Redinger for the computer program used to calculate the photoionization cross sections. This work has been supported by the Fonds zur Förderung der wissenschaftlichen Forschung in Österreich (Austrian Science Foundation) under Project No. 7192. The numerical calculations were performed on an IBM 3090–400 VF of the Computer Center of the University of Vienna, supported by the IBM European Academic Supercomputer Initiative (EASI).

[1] T. E. Faber, *An Introduction to the Theory of Liquid Metals* (Cambridge University Press, Cambridge, 1972).
[2] M. Shimoji, *Liquid Metals* (Academic, New York, 1977).
[3] N. E. Cusack, *The Physics of Structurally Disordered Matter* (Hilger, Bristol, 1987).
[4] N. F. Mott, Philos. Mag. **13**, 989 (1966).
[5] N. F. Mott, *Metal-Insulator Transitions* (Taylor and Francis, London, 1974).
[6] L. E. Ballentine, Can. J. Phys. **44**, 2533 (1966).
[7] T. Itami and M. Shimoji, Philos. Mag. **25**, 229 (1972).
[8] T. Chan and L. E. Ballentine, Can. J. Phys. **50**, 813 (1974).
[9] A. B. van Oosten and W. Geertsma, Physica B **133**, 55 (1985).
[10] J. Hafner, S. S. Jaswal, M. Tegze, A. Pflugi, J. Krieg, P. Oelhafen, and H. J. Güntherodt, J. Phys. F **18**, 2583 (1988).
[11] P. Oelhafen, G. Indlekofer, and H. J. Güntherodt, Z. Phys. Chem. **157**, 483 (1988).
[12] G. Indlekofer, P. Oelhafen, R. Lapka, and H. J. Güntherodt, Z. Phys. Chem. **157**, 465 (1988).
[13] G. Indlekofer and P. Oelhafen, Proceedings of the Seventh International Conference on Liquid and Amorphous Metals [J. Non.-Cryst. Solids **117&118**, 340 (1990)].
[14] S. S. Jaswal and J. Hafner, Phys. Rev. B **38**, 7311 (1988).
[15] J. Hafner and S. S. Jaswal, Phys. Rev. B **38**, 7320 (1988).
[16] W. Jank and J. Hafner, Europhys. Lett. **7**, 623 (1988).
[17] W. Jank and J. Hafner, Phys. Rev. B **41**, 1497 (1990).
[18] J. Hafner and M. C. Payne, J. Phys. Condens. Matter **2**, 221 (1990).
[19] R. Car and M. Parrinello, Phys. Rev. Lett. **55**, 2471 (1985).
[20] M. C. Payne, P. D. Bristow, and J. D. Joannopoulos, Phys. Rev. Lett. **58**, 1348 (1987).
[21] R. Car and M. Parrinello, Phys. Rev. Lett. **60**, 204 (1988).
[22] I. Stich, R. Car, and M. Parrinello, Phys. Rev. Lett. **63**, 2240 (1989).
[23] M. Tegze and J. Hafner, J. Phys. Condens. Matter **1**, 8293

(1989).
[24]W. A. Harrison, *Pseudopotentials in the Theory of Metals* (Benjamin, New York, 1966).
[25]V. Heine and D. Weaire, Solid State Phys. **24**, 247 (1970).
[26]J. Hafner, *From Hamiltonians to Phase Diagrams*, Vol. 70 of *Springer Series in Solid-State Sciences* (Springer, Berlin, 1987).
[27]P. Vashishta and K. S. Singwi, Phys. Rev. B **6**, 875 (1972); S. Ichimaru and K. Utsumi, *ibid.*, **24**, 7385 (1981).
[28]J. Hafner and V. Heine, J. Phys. F **13**, 2479 (1983).
[29]N. W. Ashcroft, Phys. Lett. **23**, 48 (1966).
[30]J. Hafner, in *Cohesion and Structure*, edited by D. G. Pettifor and F. R. de Boer (North-Holland, Amsterdam, 1989), Vol. 2.
[31]J. Hafner and G. Kahl, J. Phys. F **14**, 2259 (1984).
[32]J. A. Moriarty, Phys. Rev. B **8**, 1338 (1973); **6**, 4445 (1972).
[33]J. A. Moriarty, Phys. Rev. B **34**, 6738 (1986).
[34]J. A. Moriarty, Phys. Lett. A **131**, 41 (1988).
[35]U. von Barth, L. Hedin, and J. F. Janak, Phys. Rev. B **12**, 1257 (1975).
[36]J. Hafner and V. Heine, J. Phys. F **16**, 1429 (1986).
[37]J. A. Moriarty, Phys. Rev. B **28**, 4818 (1983).
[38]H. L. Skriver, Phys. Rev. B **31**, 1909 (1985).
[39]J. A. Moriarty, Phys. Rev. Lett. **55**, 1502 (1985); Phys. Rev. B **38**, 3199 (1988).
[40]J. M. Wills and W. A. Harrison, Phys. Rev. B **29**, 5486 (1984).
[41]C. Hausleitner and J. Hafner, J. Phys. F **18**, 1025 (1988).
[42]C. Hausleitner and J. Hafner, Phys. Rev. B **42**, 5863 (1990).
[43]A. Arnold, N. Mauser, and J. Hafner, J. Phys. Condens. Matter **1**, 965 (1989).
[44]A. Arnold and N. Mauser, Comput. Phys. Commun. **59**, 267 (1990).
[45]W. Knoll, in *Liquid Metals 1977*, edited by R. Evans and D. A. Greenwood (The Institute of Physics, Bristol, 1977), p. 117.
[46]A. V. Romanova, O. I. Slukhovskii, and M. Yurish, Ukr. Fiz. Zh. **23**, 722 (1978).
[47]K. S. Vahvaselkä, Phys. Scr. **18**, 266 (1978).
[48]C. N. J. Wagner, *Liquid Metals 1977* (Ref. 45), p. 110.
[49]Y. Waseda and W. A. Müller, Phys. Status Solidi B **91**, 141 (1979).
[50]M. S. Zel and B. Steffen, J. Phys. Chem. **81**, 919 (1977).
[51]Y. Waseda and K. Yokoyama, Z. Naturforsch. **30A**, 801 (1975).
[52]Y. Waseda, *The Structure of Non-Crystalline Materials—Liquids and Amorphous Solids* (McGraw-Hill, New York, 1980).
[53]O. K. Andersen, O. Jepsen, and D. Glötzel, in *Highlights of Condensed Matter Theory*, edited by F. Bassani, F. Fumi, and M. P. Tosi (North-Holland, Amsterdam, 1985).
[54]H. L. Skriver, *The LMTO Method*, Vol. 41 of *Springer Series in Solid-State* (Springer, Berlin, 1984).
[55]A. Baldereschi, Phys. Rev. B **7**, 5212 (1973); H. J. Monkhorst and J. D. Pack, *ibid.*, **13**, 5188 (1976).
[56]G. Indlekofer, Ph.D. thesis, University of Basel, 1987 (unpublished).
[57]R. Evans, D. A. Greenwood, and P. Lloyd, Phys. Lett. **35A**, 57 (1971).
[58]H. L. Skriver, Phys. Rev. Lett. **49**, 1768 (1982).
[59]Y. Chen, K. M. Ho, and B. M. Harmon, Phys. Rev. B **37**, 283 (1988).
[60]T. Jarlborg and P. O. Nilson, J. Phys. C **12**, 265 (1979).
[61]H. Winter, P. J. Durham, and G. M. Stocks, J. Phys. F **14**, 1047 (1984).
[62]J. Redinger, P. Marksteiner, and P. Weinberger, Z. Phys. B **63**, 321 (1986).
[63]W. Jank and J. Hafner, J. Phys. Condens. Matter **2**, 5065 (1990).
[64]A. M. McDonald, J. M. Daams, S. H. Vosko, and D. D. Koelling, Phys. Rev. B **23**, 6377 (1981).
[65]A. M. McDonald, J. M. Daams, S. H. Vosko, and D. D. Koelling, Phys. Rev. B **25**, 713 (1982).
[66]F. J. Himpsel, D. E. Eastman, E. E. Koch, and A. R. Williams, Phys. Rev. B **22**, 4604 (1980).
[67]M. R. Norman, Phys. Rev. B **29**, 2956 (1984).